OPTIMIZATION AND NONDETERMINISTIC ANALYSIS WITH LARGE SIMULATION MODELS: ISSUES AND DIRECTIONS

Vicente J. Romero
Thermal Sciences Dept. 9113
Sandia National Laboratories*
Albuquerque, New Mexico 87185

ABSTRACT

Economic and political demands are driving computational investigation of systems and processes like never before. It is foreseen that questions of safety, optimality, risk, robustness, likelihood, credability, etc. will increasingly be posed to computational modelers. This will require the development and routine use of computing infrastructure that incorporates computational physics models within the framework of larger "meta-analyses" involving aspects of optimization, nondeterministic analysis, and probabilistic risk assessment.

This paper describes elements of an ongoing case study involving the computational solution of several meta-problems in optimization, nondeterministic analysis, and optimization under uncertainty pertaining to the surety of a generic weapon safing device. The goal of the analyses is to determine the worst-case heating configuration in a fire that most severely threatens the integrity of the device. A large, 3-D, nonlinear, finite element thermal model is used to determine the transient thermal response of the device in this coupled conduction/radiation problem. Implications of some of the numerical aspects of the thermal model on the selection of suitable and efficient optimization and nondeterministic analysis algorithms are discussed.

1. INTRODUCTION AND OBJECTIVE OF CASE STUDY

Thermally induced failures and indeterminacies in high-consequence structures and systems, such as aircraft, weapon systems, naval vessels, petrochemical processing plants, etc., put people and engineered systems at risk. It is highly desirable to design such systems so that the risk of fire-triggered catastrophes is mitigated. This requires probing the thermal robustness of candidate designs in various credible thermal environments.

In today's computing environment, experimentally validated computer models of the behavior of such systems can be combined with optimization and sensitivity/uncertainty assessment procedures to assess robustness in a systematic manner. Answers to system- and management-level questions are being sought from computer simulation: What is the optimal solution? How robust is this optimum to uncertainties? What is the level of risk involved? What are the sensitivities and uncertainties and their implications? What are the economics of the trade-offs?

This paper illustrates the application of some advanced computational tools to assess the robustness of a conceptual weapon safing device in severe thermal environments. As well as helping expose and quantify vulnerabilities in systems, these computational tools can be used in design and resource allocation processes to build safer, more reliable, and economical (overall more optimal) systems.

2. PROBLEM DESCRIPTION

Safing Device Operation and Reliability Measure

Figure 1 shows a symmetric half of a conceptual design of a safing device in a weapon system. As explained in Reference [1], the "stronglink" component in the center of the device prevents the transfer of unauthorized electrical signals to critical components in the weapon system. In any operational or abnormal environment it must serve its standoff function until other components necessary for detonation are irreversibly neutralized. In particular, the annular capacitor winding along the outside wall of the device must become incapable of holding an electrical charge before the stronglink succumbs. The capacitor is therefore also referred to as a "weaklink".

From a thermal perspective, failure criteria for the weak and strong links is defined in terms of failure temperatures that can, in general,

*This work was supported by the United States Department of Energy under Contract DE-AL04-94AL8500. This paper is declared a work of the U.S. Government and is not subject to copyright protection in the U.S.

DISCLAIMER

be complex functions of temperature history, heating rate, geometry, boundary conditions, etc. Under thermal conditions of worst-case heating, the status of the stronglink is deemed indeterminate when certain elements on the underside of the stronglink plate shown reach 1100° F (~600° C). For the weaklink capacitor the failure criterion is taken to be the attainment of a dielectric melt temperature of 480° F anywhere on the capacitor winding.

A measure of the reliability of the safing device in any particular thermal environment is the associated "safety margin":

$$S = t\_fail_{stronglink} - t\_fail_{weaklink,} \quad \text{(EQ 1)}$$

where $t\_fail_{stronglink}$ is the elapsed time (from time zero at the beginning of a given thermal simulation) required for the hottest node anywhere on the underside of the stronglink plate to reach a failure temperature of 1100° F, and $t\_fail_{weaklink}$ is the time required for the hottest node anywhere on the capacitor winding to reach a failure temperature of 480° F. A negative safety margin indicates that the device may function unreliably.

Potentially Threatening Two-Parameter Heating Configuration

Certainly, those environments that heat the stronglink preferentially relative to the weaklink are of concern to the reliable functioning of the safing device, *i.e.*, they tend to decrease $t\_fail_{stronglink}$ relative to $t\_fail_{weaklink}$, thus decreasing the safety margin according to EQ 1. It is apparent that intense heating applied to the roof of the firing set, localized to a region directly above the stronglink plate, heats the stronglink preferentially. It is certainly plausible that an accident occurs in which a fire irradiates a circular spot on the top of the safing device; the rest of the device being essentially shaded from it. For simplicity and to maximize the localization of heating in the problem, the limiting case is assumed where the device is completely insulated everywhere except for a circular irradiated region that fully views the fire (view factor to the fire = 1.0). The size and location of the circular region of irradiation are retained as free parameters in the problem.

Thermal Model

The hydrocarbon fuel fire is modeled as a blackbody radiator at a temperature of 1000° C (1832° F). (Work is currently underway at Sandia National Laboratories to improve estimates of effective fire temperatures [2].) From geometrical and heat transfer considerations, it can be concluded that the circular region of heating should be centered on the diametral line corresponding to the plane of symmetry of the device. Thus a plane of symmetry exists in the total thermal problem {geometry + boundary conditions}, and only half of the device need be modeled. This reduces the size of the numerical radiation problem by a factor of about 3 for the given geometry and discretization. As it is, over 1800 conduction finite elements exist in the model, with a system of 7 enclosures (1046 radiation surfaces total) used to account for diffuse-gray radiant exchange within the firing set (emissivity = 0.65, representative of fire-oxidized stainless steel). The initial temperature in the simulations is always 25° C, and the fire temperature is ramped from 25° C to 1000° C over the first 10 seconds of the simulation (and held constant thereafter).

Because of the high temperatures involved, thermal radiation is extremely important in the problem. Radiative transport is a very nonlinear and computationally demanding problem to solve. Additionally, the highly temperature-dependent properties of stainless steel and the large temperature excursions involved contribute to the nonlinearity in the coupled conduction/radiation problem. Simulations required CPU times on the order of 1 hour with a dedicated 85-mhz SUN Sparkstation 20. A more detailed discussion of the computational nature of this heat transfer problem is presented in Reference [1].

Example Simulation Results

Figures 1 and 2 show results of a simulation run with the thermal model for a sample parameter set $r = 1.020$ inches = fire radius, and $x = 0.142$ inches = distance from the center of the firing set in the positive x direction as shown in Figure 2. These values define a region on the roof of the device designated by the white arrows in Figure 1. High temperatures are concentrated about the stronglink plate, but the capacitor winding is relatively cool. This combination of parameters results in a highly localized heating configuration that preferentially heats the stronglink to a high degree. Figure 2 shows the relevant weaklink and stronglink temperature responses over time. For the stated parameters, the value of the safety margin S is approximately 56 minutes.

3. WORST-CASE HEATING CONFIGURATION BY OPTIMIZATION ON NOISY DATA

What, if any, credible abnormal environments cause the race to be won or nearly won by the stronglink (and thus threaten the reliability of the safing device)? Can the worst-case environment be identified so that the device can be hardened against it?

Optimization procedures can be used to identify heating configuration parameters r and x that maximize the preferential heating of the stronglink (or, equivalently, minimize the safety margin). Reference [1] describes implementational details such as parameterizing the heat flux boundary condition in terms of r and x and adaptively stopping simulations when enough information is produced. The optimization problem is complicated by numerical artifacts resulting from discrete approximation and finite computer precision (*i.e.,* numerical noise in the objective function as discussed below), as well as theoretical difficulties associated with navigating to a global minimum on a nonconvex design surface having a fold and several local minima as described in [1].

Several different optimization procedures have already been applied to this problem with varying levels of success as described in [3]. Importantly, the most successful of these have revealed the vulnerability of the device to be an order of magnitude greater than *ad hoc* searching had previously indicated. However, the computational expense, and in many cases failure of the established searching and optimization procedures tried[1], indicates a vital need to approach such optimizations more effectively.

[1] These include conjugate gradient and Newton-based nonlinear programming methods, genetic algorithms, coordinate pattern-search methods, and Monte Carlo sampling, all invoked through Sandia's DAKOTA[4] C++ software iterator framework.

Accordingly, recent research at Sandia has been aimed at accomplishing effective optimization in the presence of noisy objective functions derived from expensive simulations with large complex computer models. Some of the issues and lessons from this work, important because such computer models will increasingly be used for policy and decision making in the future, are discussed below.

Characterization of Numerical Noise and Bias vs Temporal Discretization in the Model

To begin, the simulation CPU times and numerical inaccuracies associated with discrete time-integration and boundary conditions in the thermal model are examined. The purpose here is not to look at convergence of the solution *per se*, but ultimately to look at the relative effects of variously converged solutions on accuracy and computational expense in the overriding optimization problem.

Convergence parameters EPSIT and EPSIT2 control the iterative time-stepping procedure in the QTRAN[5] thermal model. Table 1 lists values of the per-timestep iterative convergence tolerances for the various designations 'loose', 'low', 'xstrict', etc. The CPU times in the table are averages over nine QTRAN simulations run at the parameter pairs indicated in Table 2. The parameter sets comprise a 2-D lattice of points centered on the worst-case heating parameters $\{r,x\}$ = {1.6204 in., 0.78205 in.} identified in [1] at xstrict tolerances. The significance of this lattice of design points will become apparent later. The CPU times were obtained on a dedicated 85-mhz SUN Spark20 workstation. The 'xstrict' simulations are on average over 17 times more expensive than 'xloose' simulations.

Table 1 Per-Timestep QTRAN[5] Convergence Tolerance Settings and Associated Simulation Time Requirements

Case	EPSIT tolerance	EPSIT2 tolerance	Avg. CPU time (min.)	% of 'xstrict' time
xstrict	$1x10^{-4}$	$1x10^{-6}$	174.0	100.0%
low	$1x10^{+0}$	$1x10^{-2}$	20.7	11.9%
loose	$1x10^{+1}$	$1x10^{-1}$	14.2	8.2%
xloose	$1x10^{+2}$	$1x10^{-0}$	10.1	5.8%

Figure 3a plots a 1-D parameter study of the behavior of the objective function versus discrete increments in the fire radius r for various degrees of temporal resolution in the thermal model. The study is centered about the optimal worst-case heating parameters. Similar noise exists along the x direction (see [6]), though results are not shown here to conserve space[2].

[2] It would also be instructive to investigate the nature of noise for various levels of spatial discretization (i.e., mesh or element size), though no work has been done toward this purpose for the current thermal model.

Table 2 9-Point Grid in 2-D optimization space, centered on point corresponding to deterministic worst-case heating

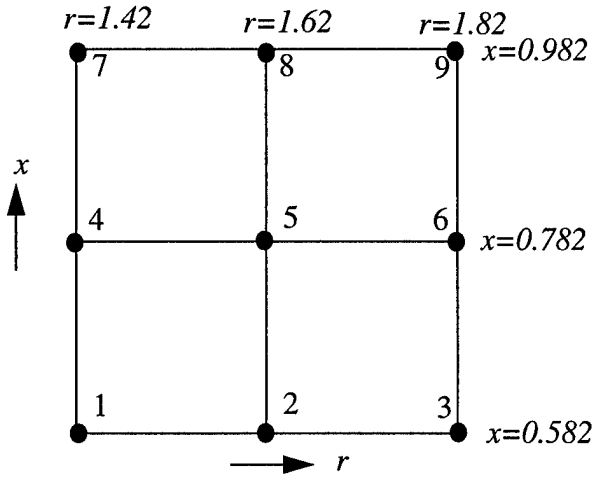

A significant aggregate downward shifting or "bias" in the results also occurs as the tolerance parameters EPSIT and EPSIT2 are loosened. This is perhaps due to a retarding of thermal diffusion in the model under the bigger timesteps allowed by looser per-timestep convergence tolerances. The response lag of the more thermally buried weaklink would then increase, resulting in a lower safety margin. Though the absolute values of the safety margins for the 'xloose' runs are on the order of 20% lower than those for the 'xstrict' runs, the overall shapes of the parameter study curves are fairly close, which is the important quality in optimization.

As shown later, numerical noise and bias from Monte Carlo nonconvergence and other numerical operations arising in optimization under uncertainty (OUU) amplifies the need to develop and use noise-tolerant optimization strategies.

Optimization in the Presence of Numerical Noise

The spacing of the data points in the parameter study is 0.005 inch, which is on the same order as the 0.003 in. to 0.005 in. spacing in previous parameter studies of noise in [3] and is compatible with the physical finite-difference step sizes of approximately 0.001 inch in the final optimization runs therein. Therefore, the noise displayed in Figure 3a is comparable to the noise experienced by the optimizers in the previously published studies. As the plot shows, the objective function at 'xstrict' tolerances is very smooth, which allowed DAKOTA's DOT[7] conjugate-gradient optimizer to find the optimal design parameters. The care taken to parameterize the heat flux boundary condition as a smooth and continuous function of r and x is evident in the 'xstrict' data. However, a discernable, though not directly consistent, relationship exists between temporal discretization in the numerical model and the spatial correlation of the data. The numerical anomalies evident for the less strict per-timestep error tolerances result in local sub-minima that can trap or confuse derivative-based optimizers as was seen in [1], even though on an absolute scale the perturbations (usually well within 10% of the

projected unperturbed results) are acceptably small for most engineering purposes.

Optimization in the presence of "small-scale"[3] stochastic noise, as may arise from finite numerics due to truncation, discretization, machine roundoff, etc., in computational physics models, does not appear to have been addressed much in the literature to date. However, nontrivial numerical noise has also shown up in many other optimization problems recently studied at Sandia (see *e.g.*, [8]). We now demonstrate a simple approach to optimization in the presence of stochastic numerical noise.

The idea is to step out of the scale of the noise by taking large enough perturbations or optimization step sizes to get effective low-order function approximations that locally reflect only the relevant macrotopology in the problem. Classical optimization techniques are then used to quickly converge to optima on the analytic (noise-free) objective functions. If the noise level in the data approaches the scale of the macrotopology in the optimization problem, then the current computational model must be replaced with a more finely discretized one in order to profitably pursue the optimization process. *This approach should be viewed as one that, rather than operating from local gradients built from small-perturbation differencing in the parameter space, instead samples more broadly to build local interpolation surfaces with analytically defined derivatives that can be quickly and easily navigated with classical derivative-based optimization techniques.* This simple local optimization scheme is used as the innermost loop in a more complex multi-level, iterative, adaptive, and convergence self-assessing procedure being devised at Sandia for efficient global optimization in the presence of noise.

"Macro curve" representations obtained by fitting quadratic functions through the left-most, center, and right-most points of the data in Figure 3a are plotted in Figure 3b. Despite the stochastic noise in the lower-tolerance data, their quadratic representations exhibit overall *relative* topologies that resemble very closely that of the 'xstrict' data, as established quantitatively in [6]. *Though the lower-tolerance macro curves are in aggregate vertically shifted somewhat from the 'xstrict' macro curve, the* ***relative*** *topologies are similar, which is what is most important in optimization.* Furthermore, *achieving accuracy in prediction of relative macro behavior is fairly inexpensive; e*ven the simulations with xloose tolerances produce topologies very similar to those based on xstrict tolerances, but on average take 1/17 the CPU time.

Certainly, optimization of smooth, continuous design surfaces (which is the bulk of the applications in engineering) depends on **relative** information, as opposed to **absolute** information. *This relaxes the demands on simulation models used in optimization from a "strong" requirement of having to provide good absolute information to a much weaker requirement of having to simply provide good relative information.* (Here terminology is drawn from the finite element literature, where "strong" and "weak" solutions of differential equations are spoken of, the later being more easily obtainable because of reduced requirements on the solution.) As we have already seen and will see more evidence of in the following, such relative information can be obtained relatively inexpensively with physics-based models. Therefore, *large-scale optimization with complex simulation models can be made much more affordable by realizing the savings resident in the weakened requirements on the simulation models.* However, the tradeoff between model fidelity (*i.e.*, resolution and therefore cost) vs. effectiveness in the context of optimization (*i.e.*, smallest scale at which macro trends are discernable above the numerical noise, and accurateness in the trends) is a much less clear-cut issue. Because numerical noise is dependent both upon the discrete resolution of the numerical model and on the region of the parameter space being operated in, the above question is not answerable *a priori*. However, it may be resolvable "on the fly" with a multi-level, multi-grid "Lattice Sampling" adaptive optimization scheme presently being investigated (see [6]).

The potential of the suggested macroscale optimization approach is clearly evident. Overall, this initial examination reveals that *a simple quadratic fit to very sparse and inexpensively produced data (from xloose tolerances) can yield points very nearly optimal in the design space.* Of course, reducing the macro scale and the coarseness of the numerical model in coordinated succession should lead to convergence to the final "target" results $\{r,x\}$ = {1.6204 in., 0.78205 in.}. This remains to be verified in future work, with special attention to be paid to the computational efficiency of this process vs. other optimization methods already tried as reported in [3].

Optimization on 4X Macro Scale Biquadratic Response Surface

For a quantitative indication of the accuracy of optima arrived at from local low-order polynomial fits to the data, we examine the results of a study at the 4X "sub-grid" macro scale on which the grid of points in Table 2 is based. The thermal model was run at each of the nine input parameter sets at each of the aforementioned tolerance levels. Figure 4 plots a quadratic bi-Lagrange polynomial fit (see [9]) through the nine data points corresponding to xstrict tolerances. (The piecewise-bilinear plot was generated by interpolating off of the biquadratic function to get an 11x11 grid of response-surface values.)

The "difference" plot in Figure 5 shows the differences between biquadratic fits of 'xloose' and 'xstrict' data on an 11x11 (121-point) grid. If the difference surface was a horizontal plane, then the 'xstrict' and 'xloose' surfaces would have exactly the same topologies, shifted vertically by the level of the difference plane. The relatively small undulation (less than 0.4 minutes over the entire range of the design space on a scale ranging from about 2.5 minutes to 25 minutes) indicates fairly similar topologies for the two levels of temporal resolution. As expected, the 'xloose' deviations bound the deviations of corresponding 'loose' and 'low' surfaces (not plotted).

The **effective** optimization similarity of the topologies of the biquadratic surfaces can be determined by comparing the coordinates of their minima. The r optima for the biquadratic surfaces at the four tolerance levels are listed in Table 3. The optima were found with the commercial nonlinear programming

[3] Of course, "small-scale" is a relative term: small scale perturbations or oscillations are those deviations from a clearly recognizable macro trend occuring at some larger scale of interest in the design problem.

optimization package NPSOL[10] of the DAKOTA[4] iterator toolkit. Because the biquadratic fits are analytic surfaces, partial derivatives of any order and mixing are available analytically for the optimization step. Only first-order analytic derivatives were supplied for this application. Starting from the coordinates at the center of the grid as an initial guess, NPSOL typically required about seven iterations, converging to the optimum in just a few CPU seconds.

Table 3 Optimal fire radius *r* from biquadratic safety margin surfaces (4X macroscale)

Tolerance	optimal *r* (in.)	% diff. from xstrict case	% diff. from target value of *r*=1.62 in [1]
xstrict	1.605	-	-0.93%
low	1.606	0.06%	-0.86%
loose	1.604	-0.06%	-0.99%
xloose	1.607	0.13%	-0.80%

Results are only from 0.8% to 1% different from the target *r* value (see Table 3). Convergence to the target optima as the sub-grid macroscale decreases is to be expected as long as the sub-grid macroscale does not drop to the scale of the simulation noise from the numerical model. A similar study reported in [6] at one-fourth the sub-grid scale confirms that 1X macroscale results differ from the target *r* value by from 0.2% to 0.7% depending on the QTRAN tolerances of the underlying data. Considering that a factor of 4 reduction in the sub-grid macroscale translates on average to somewhat less than a factor of 4 improvement in the result, the average rate of convergence in the *r* optimum is somewhat less than linear. However, similar results for the fire location parameter *x* reported in [6] show a linear rate of convergence with decreasing sub-grid macroscale.

The values in Table 3 reveal that the simple local response-surface optimization technique employed is very insensitive at the 4x macroscale to the level of temporal discretization of the numerical model. In other words, at the macroscales involved, the optimal design parameters found were essentially the same whether the nine-point basis was generated with 174 CPU-minute (on average) 'xstrict' simulations or with 10 CPU-minute (on average) 'xloose' simulations. *Certainly, a model with greater resolution is useful in the end for very local final convergence to an optimum and for a more accurate absolute valuation of the objective function there, but in early rounds of optimization this degree of resolution is unnecessary and unnecessarily costly.*

An Efficient? Global-to-Local Analytic Multigrid Optimization Strategy

Global optimization might be accomplished by covering the full parameter space of interest with many such nine-point grids and sampling the response at each grid point with a very coarse (fast-running) numerical model. Local optima would then be identified from local biquadratic fits as explained above. The discretization of the model could then be increased appropriately and the process would be repeated. If the local optima identified at the first and second levels of discretization differ within a specified tolerance, then the discretization of the models is sufficient for the sub-grid scales employed in the first round of optimization. Other rounds of optimization are then pursued with the coarse model and the smaller of the macroscales tested in the first round. In these subsequent rounds, separate nine-point grids centered about local optima identified in the first round would be pursued as separate local optimization problems, with successive decreases in each round of the sub-grid scales of the biquadratic fits involved. At each round some "active" regions may be dropped from further consideration following a relative comparison of the local optima in the remaining regions. In this way the global optimum can be converged on with a relatively noisy but inexpensive model. This process can continue until the optima identified in successive rounds of sub-grid scale reduction begin diverging, which is an indicator that the working sub-grid scale is entering a regime where the numerical noise of the simulation model begins to interfere. In this case the model's resolution must be increased if further convergence to the optimum is desired. In the future it is planned to compare variants of this basic strategy against other global optimization approaches on real problems where the objective function is comprised from noisy and expensive simulations.

4. NONDETERMINISTIC ANALYSIS

It is widely acknowledged that engineering models of systems and processes suffer from various degrees of uncertainty in material properties, geometries, operating and boundary conditions, numerical preciseness, etc. Nondeterministic analysis, which reveals the effects of uncertainties in the model, yields a much broader picture of probable behavior than nominal point estimates indicate. In fact, we find here that the effects of uncertain weaklink and stronglink failure temperatures are very significant and that a probabalistic description of the safety margin leads to a quite different conclusion than the deterministic one does.

Sensitivity of Safety Margin vs. Weaklink and Stronglink Failure Thresholds

A glance at Figure 2 indicates that stronglink and weaklink failures occur in relatively flat portions of the temperature response curves. This is more true for the stonglink than for the weaklink, but regardless it can be seen that the safety margin is very sensitive to the failure temperature criteria. Thus, non-negligible uncertainties in the failure criteria of the stronglink and weaklink will have a major impact on the uncertainty of the safety margin. In fact, as established in [11], when uncertainty bands 5% above and below the nominal failure temperatures are considered, the corresponding bands in failure times indicate that the safety margin could vary from about 34.5 minutes at best to about -25.5 minutes at worst. Comparing this to the "deterministic" safety margin of 2.53 minutes calculated with xstrict tolerances at worst-case heating parameters, it is apparent that the effects of uncertainty are very important in this problem.

Calculation of Safety Margin Distribution Due to Uncertain Component Failure Thresholds

In the following, the stronglink and weaklink failure temperatures are assumed to be described by truncated normal distributions with means μ equal to the respective mean failure temperatures of 593.33 ° C (1100 ° F) and 248.89 ° C (480 ° F). Based on some experimental data [11], standard deviations σ are taken to be 3% of the means, *i.e.* 17.8 ° C and 7.47 ° C respectively. The failure criteria standard deviations specified here would certainly seem to be reasonable for complex manufactured components like the strong and weak links. With negligible impact on the final results, the distributions are truncated at 3σ above and below their mean values for numerical convenience.

As explained more fully in Reference [12], sets of weaklink and stronglink failure temperatures can be generated from the above failure temperature distribution parameters via Latin Hypercube (LHS[13]) Monte Carlo sampling[4], and then a safety margin can be computed for each set by using the time histories of the weak and strong links obtained from a run of the thermal model under given $\{r,x\}$ heating conditions. Histogram representations of safety margin distributions obtained for the three $\{r,x\}$ parameter sets of the middle row of Table 2 are displayed in Figure 6. The results are derived from simulations with xstrict tolerances.

Recent work in "decoupling" the probabilistic and deterministic portions of uncertainty problems like this with a "decoupled" Monte Carlo technique utilizing piecewise-local finite element response surfaces built on "Lattice Sampling" is reported in [14]. This work suggests that it is generally more efficient to use model simulations to build a response surface than to use them directly in a Monte Carlo simulation. Potentially then, the Finite Element/ Lattice Sampling Decoupled Monte Carlo (FELSDMC) approach can make Monte Carlo analysis orders of magnitude less expensive with no appreciable loss in accuracy.

Whether using a direct or decoupled Monte Carlo approach, establishment of Monte Carlo convergence is a difficult issue. Moreover, there is a need for numerical tools for "on the fly" automated convergence assessment and termination of sampling when sufficient convergence within user-specified tolerances has been achieved. Algorithms for doing this are currently being devised and tested at Sandia (see *e.g.*, [15]), though robustness of the algorithms has not yet been comprehensively tested or established.

Certainly, other methods besides the direct Monte Carlo approach exist for estimating probability of failure. In fact, the simple reliability-based Mean Value (MV) method applied in [12] was effective with only 5 samples (vs. 500 with the Monte Carlo approach). The MV approach was adequate because the assumptions of the method apply quite well for the current problem: the input uncertainty distributions are normal and the temperature histories of the weak and strong links are essentially linear in the neighborhood of the failure temperatures (*cf* Figure 2).

[4] The cumulative experience at Sandia has been that the LHS Monte Carlo method is much more efficient than simple random sampling Monte Carlo methods —*i.e.*, the asymptotic rate of convergence of the population mean and standard deviation is usually significantly better.

Because the Mean Value method is not necessarily conservative and cannot be counted upon to be accurate under more general circumstances, other established approaches for probability and reliability prediction are currently being evaluated at Sandia (see [16]).

Metrics of the Safety Margin Distribution: Safing Device Reliability or Probability of Failure

Population means and percentiles are also plotted in Figure 6 and fitted with quadratic curves as shown. A quadratic curve representing the deterministic[5] safety margin is also plotted in the figure. Though the deterministic curve is relatively close to the Monte Carlo[6] mean curve and the median (50th percentile) curve, significant differences do exist. For example, the mean safety margin for the center histogram is approximately 3.16 minutes, about 25% greater than the deterministic estimate of 2.53 minutes. Thus, it is good news that the expected safety margin is actually greater than the nominal point estimate. However, two caveats exist. First, as the plot shows, the mean curve does not always lie above the nominal curve, so deterministic point estimates are not always conservative. Second, as the histogram shows, a very substantial number of Monte Carlo trials actually resulted in **negative** safety margins. Therefore the large spread in the results reveals a very substantial probability of device failure or unreliability. Indeed, a 45% chance of safing device failure exists, corresponding to the proportion of the histogram below the S=0 abscissa line in the figure.

The sensitivity of failure probability to the variance or spread in the weaklink and stronglink failure temperature distributions was also studied briefly in [11]. When the standard deviations of the input distributions were halved from 5% to 2.5% of the mean failure temperatures (with 4σ truncation), the resulting probability of failure only dropped from 0.47 to about 0.43. That the standard deviations of the input distributions were halved and the probability of failure only dropped 8.5% is not very encouraging. Thus the candidate safing device is certainly very vulnerable to even small uncertainties in failure criteria of the critical internal components under conditions of worst-case heating. *This has implications for robust design in the presence of uncertainty.*

5. OPTIMIZATION UNDER UNCERTAINTY

The predeeding section demonstrated the importance of nondeterministic effects in the current application. It is, therefore, imprudent to ignore such effects in the larger optimization problem.

Because accounting for uncertainties in weaklink and stronglink failure criteria results in a spread of safety margins rather than just

[5] The deterministic safety margin is the single point estimate of the safety margin obtained by evaluation at the nominal or mean stronglink and weaklink failure temperatures 593.33 ° C and 248.89 ° C, respectively.

[6] Based upon experience gained in [11], 500 samples are more than adequate for stabilized probability estimates for probabilities in the range 0.4 to 0.5. However, the number of samples required for results to stabilize is problem and situation dependent, so the Monte Carlo results presented here may not be completely converged.

a single value, the choice of an objective function for optimization becomes an issue. The expected (mean) value of the safety margin could be used, or the 25th percentile, or the mean plus n standard deviations, etc. Moreover, the histograms and the percentile curves in Figure 6 show that in this region of the parameter space the safety margin distribution changes fairly rapidly. Thus, the optimum point in an optimization problem could be significantly different for each potential objective function formulation. For example, the 75th percentile curve reaches a minimum at approximately r = 1.68 in., which is about 5.7% larger than the mean, median, and nominal or deterministic curve minima at approximately r = 1.59 in., which is about 5.3% larger than the 25th percentile curve minimum at approximately r = 1.51 in.

Reference [12] reports an application of optimization under uncertainty (OUU) in this problem, where the objective function is defined as the probability of safing device failure —*i.e.*, that the safety margin is less than zero. The maximum of this function then identifies the heating configuration that is the most threatening in a probabilistic sense —*i.e.*, when uncertainties in information about the system are taken into account. Thus, it speaks to the robustness of the system in a real-world setting where exact information about the problem is not possessed or cannot be modeled. Particular attention is paid in [12] to how nondeterministic analysis affects the noisiness of the objective function, which in turn fundamentally affects the effectiveness and applicability of optimization algorithms and therefore the user's selection of an optimization strategy. Figure 7 shows a parameter study of noise in the probabilistic objective function induced by Monte Carlo and Mean Value approaches. The 'mc.prob.xstrict' and 'mv.prob.xstrict' curves correspond to the (smooth) 'xstrict' objective function in Figure 3a. The Monte Carlo process clearly induces more noise into the objective function than the Mean Value process does. It is currently being determined whether the Monte Carlo noise is due to nonconvergence or not, and, therefore, how adaptive sampling with a MC convergence-testing tool ([15]) might smooth the objective function in OUU problems. Despite the noise, the response-surface approach described in Section 3 was applied in [12] to the OUU problem with very encouraging results.

6. CONCLUSION

Enabled by accelerating computational capability, a new generation of very powerful analysis tools are becoming available to engineers for affecting system-level decisions with multi-point analysis. Such system analyses couple high-fidelity physics simulations with higher-level optimization, probabilistic risk assessment, and nondeterministic analysis drivers. Thus, computers are being used to help answer broader questions of robust design, probabilistic behavior, reliability, etc. Application of these analysis methods will become routine engineering practice in the future, but much enabling progress still remains to be made in efficient adaptive and hybrid methodologies for effectively handling noisy data from large simulation models and processes. Some steps in this direction are reported on here.

7. REFERENCES

[1] Romero, V.J., Eldred, M.S., Bohnhoff, W.J., and Outka, D.E., "Application of Optimization to the Inverse Problem of Finding the Worst-Case Heating Configuration in a Fire," Numerical Methods in Thermal Problems, Vol. IX, Part 2, pp. 1022-1033, Pineridge Press, R.W. Lewis and P. Durbetaki, eds., Proceedings of the 9th Int'l. Conf. on Numerical Methods in Thermal Problems, Atlanta, GA., July 17-21, 1995.

[2] Gritzo, L.F., and Nicolette, V.F., "Coupled Thermal Response of Objects and Participating Media in Fires and Large Combustion Systems," Numerical Heat Transfer, - Part A, no. 28, 1995, pp. 531-545.

[3] Eldred, M.S., Hart, W.E., Bohnhoff, W.J., Romero, V.J., Hutchinson, S.A., and Salinger, A.G., "Utilizing Object-Oriented Design to Build Advanced Optimization Strategies with Generic Implementation," proceedings of the Sixth Multi-Disciplinary Optimization Symposium, Belleview, WA, Sept. 4-6 1996.

[4] DAKOTA User Manual, Sandia National Laboratories report SANDxx.xxxx (in progress)

[5] P/THERMAL Analysis Package User Manuals, Release 2.6, March 1993, PDA Engineering, Costa Mesa, CA.

[6] Romero, V. J., "Noise and Bias vs. Model Resolution in Complex Physics Simulations and a Simple Response Surface Approach for Making Numerical Optimization More Affordable," submitted to Computer Modeling and Simulation in Engineering

[7] DOT Users Manual, Version 4.10, VMA Engineering, Colorado Springs, CO, 1994.

[8] Eldred, M.S., Outka, Bohnhoff, W.J., Witkowski, W.P., Romero, V.J., Ponslet, E.J., and Chen, K.S., "Optimization of Complex Mechanics Simulations with Object-Oriented Software Design," in Computer Modeling and Simulation in Engineering, Vol. 1 No. 3, August, 1996, pp. 323-352.

[9] Hughes, Thomas J.R., "*The Finite Element Method Linear Static and Dynamic Finite Element Analysis*", Prentice-Hall, Inc., A Division of Simon & Schuster Englewood Cliffs, NJ, 1987.

[10] Gill, P.E., Murray, W., Saunders, M.A., and Wright, M.H., "User's Guide for NPSOL (Version 4.0): A Fortran Package for Nonlinear Programming," System Optimization Laboratory, TR SOL-86-2, Stanford University, Stanford, CA, Jan. 1986.

[11] Romero, V. J., "Making Use of Optimization, Nondeterministic Analysis, and Numerical Simulation to Assess Firing Set Robustness in a Fire," Proceedings of the 14th Int'l. System Safety Conference, Aug. 12-

17, 1996, Albuquerque, New Mexico, System Safety Society - publisher, Sterling, VA., pp. 5D4-1-5D4-11.

[12] Romero, V.J., Painton, L.A., and Eldred, M.S., "Optimization Under Uncertainty: Accounting for uncertain component failure thresholds in finding the worst-case heating on a safing device," in preparation for submission to Computer Modeling and Simulation in Engineering journal

[13] Iman, R.L., and Shortencarier, M.J., "A FORTRAN77 Program and User's Guide for the Generation of Latin Hypercube and Random Samples to Use with Computer Models," Sandia National Laboratories report SAND83-2365 (RG), printed March 1984.

[14] Romero, V. J., and Bangston, S. D., "Efficient Monte Carlo Probability Estimation with Finite Element Response Surfaces built from Progressive Lattice Sampling," submitted to the joint AIAA/ASME/ASCE/AHS/ASC 39th Structures, Structural Dynamics, and Materials (SDM) Conference, April 20-23, 1998, Long Beach, California.

[15] Chen, K. S., and Romero, V. J., "An Automated Convergence Assessment Algorithm for Adaptive Termination of Monte Carlo Sampling with Application to Several Example Problems," Sandia National Laboratories report in preparation.

[16] Romero, V. J., "Efficient Propagation of Uncertainty and Probabilistic Behavior through Engineering Models via Decoupled Monte Carlo with Finite Element Response Surfaces Built from Structured Sampling," in preparation for submission to International Journal for Numerical Methods in Engineering

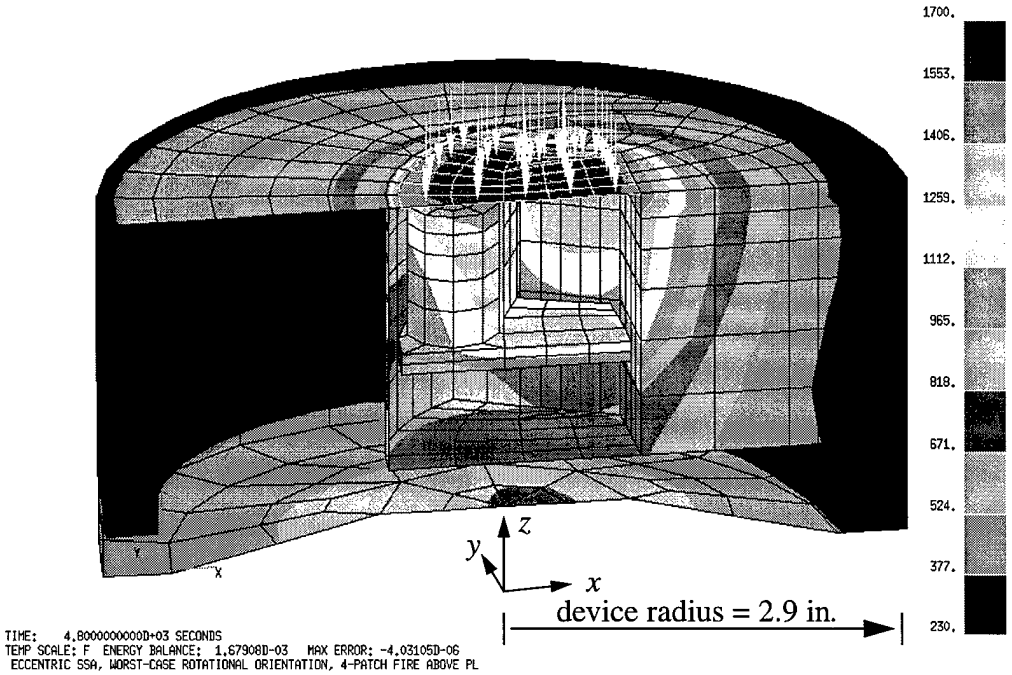

Figure 1 Safing device temperature distribution ($^{\circ}$F) 80 minutes after the start of the fire, heating parameters r=1.02 in., x=0.142 in.

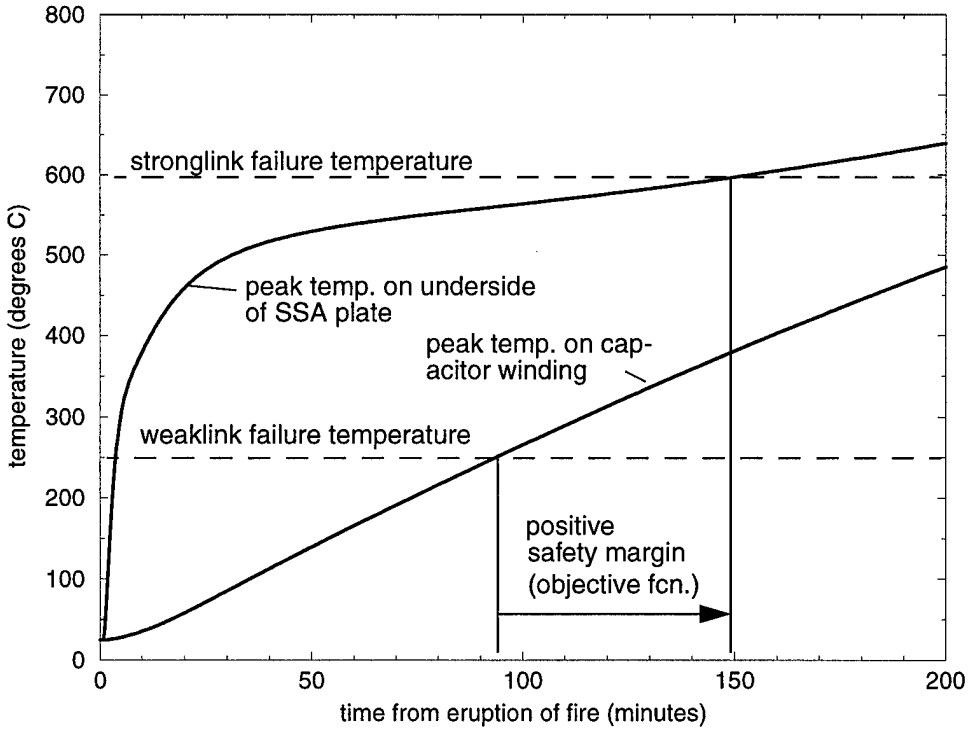

Figure 2 Stronglink and weaklink temperature histories for r=1.02 in., x=0.142 in.

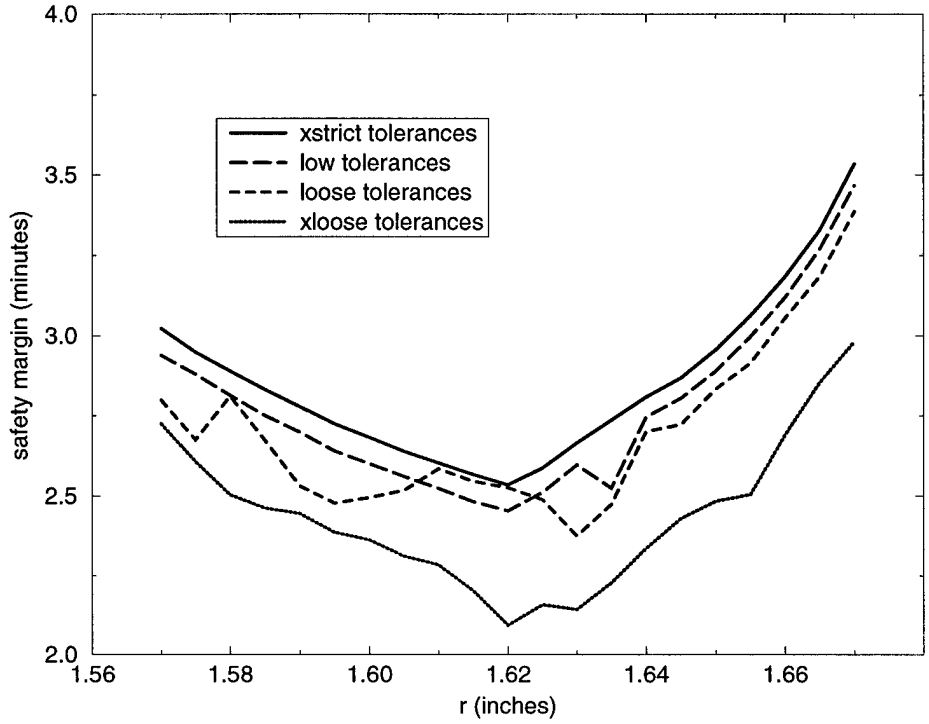

Figure 3a Numerical noise along r for deterministic objective function in the vicinity of the deterministic optimum (x=0.782 in.) for various QTRAN convergence tolerance settings.

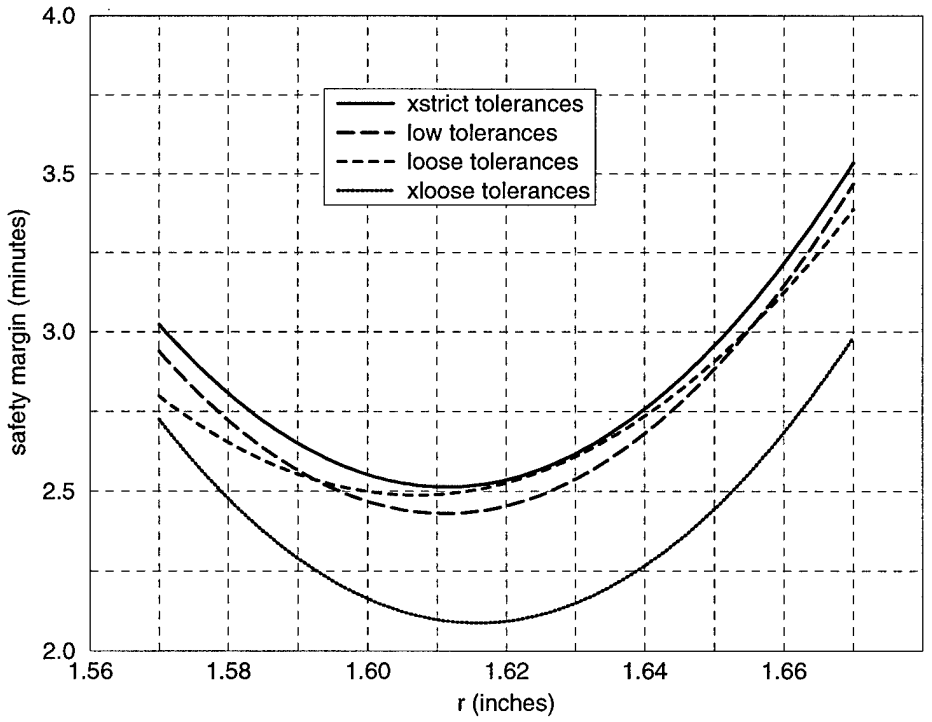

Figure 3b Quadratic "macro curves" in the r direction in the vicinity of the deterministic optimum (x=0.782 in.) for various QTRAN convergence tolerance settings.

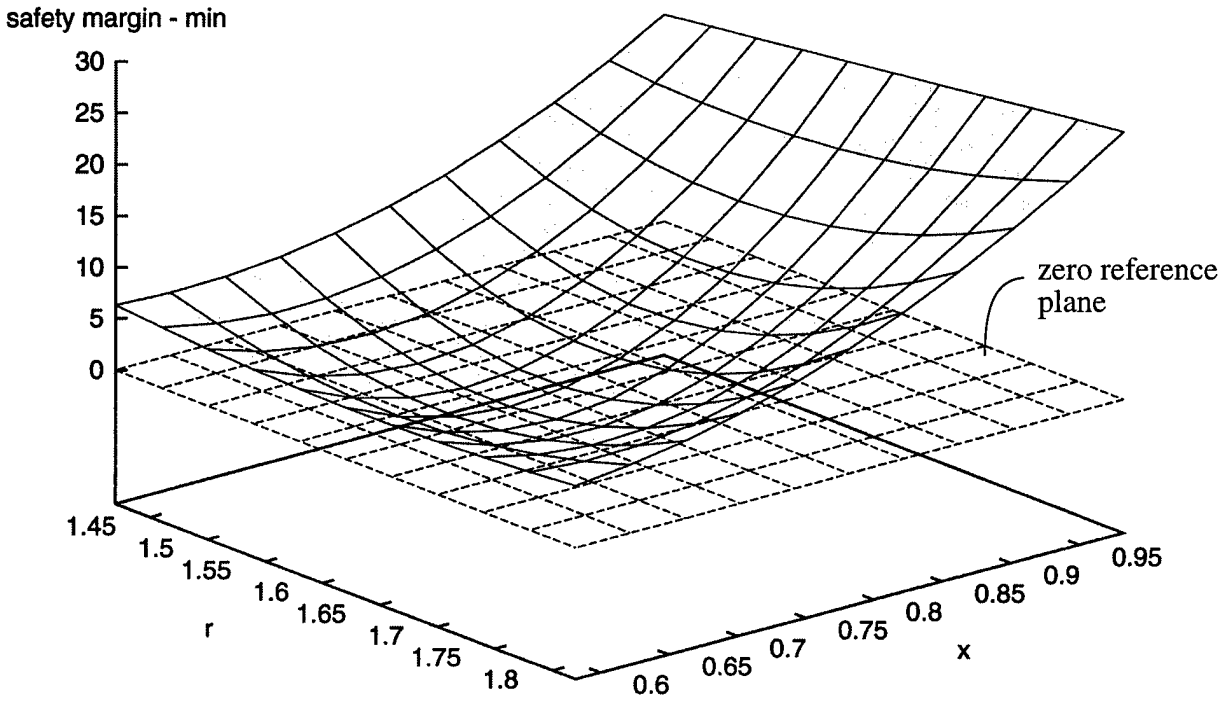

Figure 4 Safety margin response surface (objective function for deterministic optimization problem) from biquadratic fit to 'xstrict' responses at the nine grid points shown in Table 2.

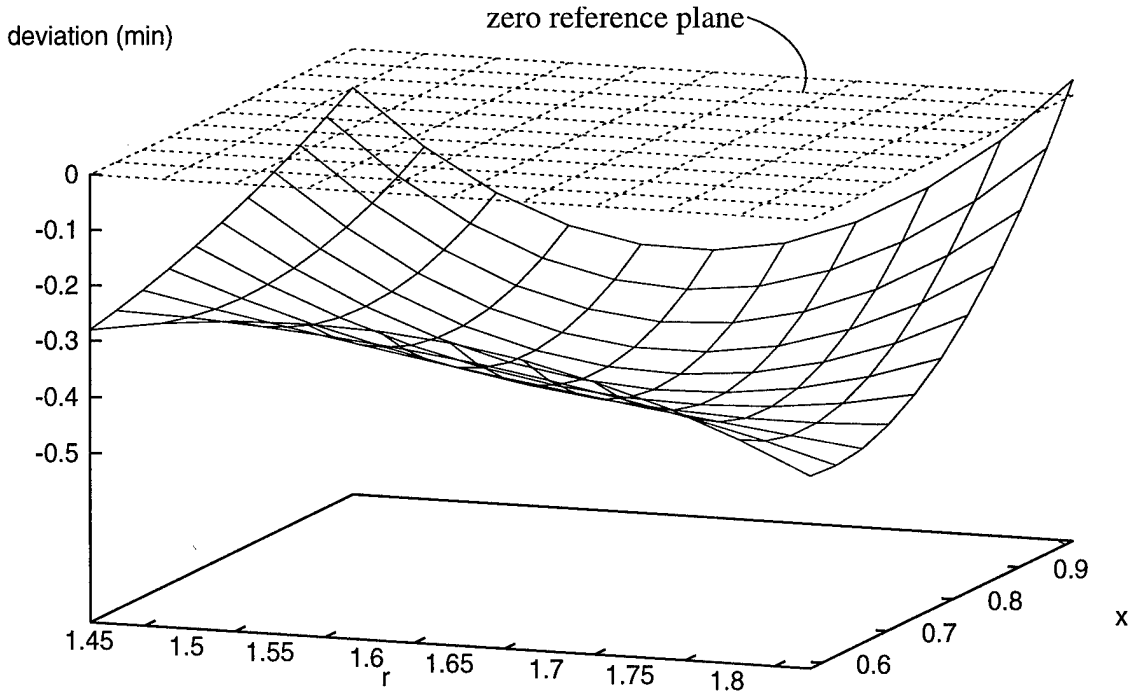

Figure 5 Difference plot showing deviation of 'xloose' biquadratic response surface from biquadratic surface fit to 'xstrict' data at the nine grid points.

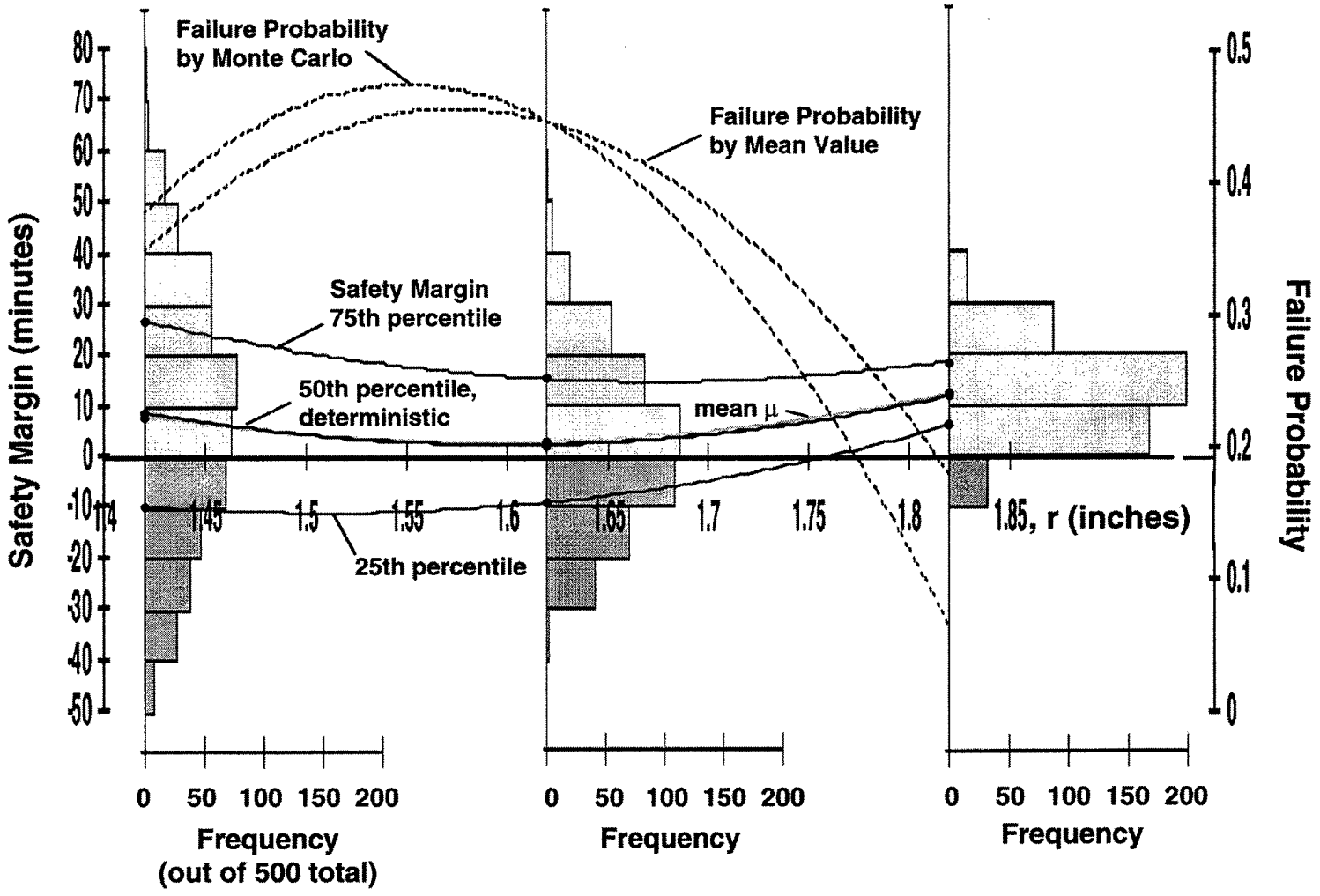

Figure 6 Implications of including uncertain component failure thresholds in the formulation of the optimization problem.

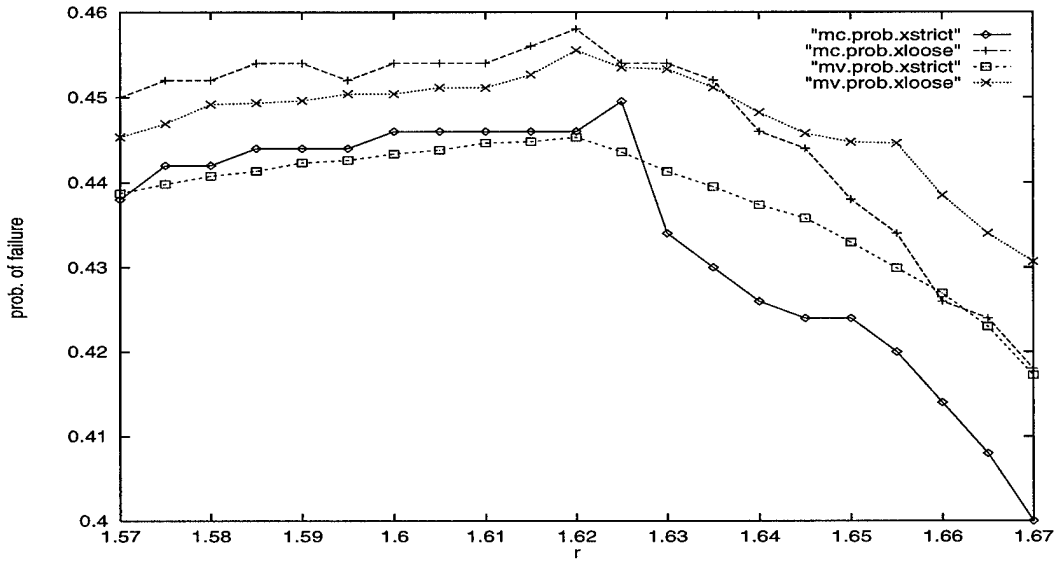

Figure 7 Numerical noise along r in the vicinity of the deterministic optimum (x=0.782 in.) for probabalistic objective functions based on various tolerance settings and probability calculation methods.

Report Number (14) SAND--98-1285C
CONF-980610--

Publ. Date (11) 199806
Sponsor Code (18) DOE/DP, XF
UC Category (19) UC-700, DOE/ER

DOE